

Assessment of a stochastic downscaling methodology in generating an ensemble of hourly future climate time series

S. Fatichi · V. Y. Ivanov · E. Caporali

Received: 29 January 2012 / Accepted: 5 December 2012 / Published online: 22 December 2012
© Springer-Verlag Berlin Heidelberg 2012

Abstract This study extends a stochastic downscaling methodology to generation of an ensemble of hourly time series of meteorological variables that express possible future climate conditions at a point-scale. The stochastic downscaling uses general circulation model (GCM) realizations and an hourly weather generator, the Advanced WEather GENERator (AWE-GEN). Marginal distributions of factors of change are computed for several climate statistics using a Bayesian methodology that can weight GCM realizations based on the model relative performance with respect to a historical climate and a degree of disagreement in projecting future conditions. A Monte Carlo technique is used to sample the factors of change from their respective marginal distributions. As a comparison with traditional approaches, factors of change are also estimated by averaging GCM realizations. With either approach, the derived factors of change are applied to the climate statistics inferred from historical observations to re-evaluate parameters of the weather generator. The re-parameterized generator yields hourly time series of meteorological variables that can be considered to be representative of future climate conditions. In this study, the time series are

generated in an ensemble mode to fully reflect the uncertainty of GCM projections, climate stochasticity, as well as uncertainties of the downscaling procedure. Applications of the methodology in reproducing future climate conditions for the periods of 2000–2009, 2046–2065 and 2081–2100, using the period of 1962–1992 as the historical baseline are discussed for the location of Firenze (Italy). The inferences of the methodology for the period of 2000–2009 are tested against observations to assess reliability of the stochastic downscaling procedure in reproducing statistics of meteorological variables at different time scales.

keywords Stochastic downscaling · Weather generator · Uncertainty assessment · Firenze · Italy

1 Introduction

Research studies of climate change impacts at the local scales of human management and for specific environmental applications, e.g., water resources, ecosystem services, agricultural productivity, etc., are growing exponentially (e.g., Christensen et al. 2004; Ines and Hansen 2006; Bae et al. 2008; Bavay et al. 2009; Mooney et al. 2009; Manning et al. 2009; Morin and Thuiller 2009; Hirschi et al. 2012); see also Fowler et al. 2007a and Maraun et al. 2010 for recent reviews. A necessary step in such studies is “downscaling” of climate projections, i.e., a transfer of information content of climate model realizations to the spatial and/or temporal scales that are finer than the original model output. Most of the techniques that have been presented in downscaling General Circulation Model (GCM) realizations have targeted regional spatial scales at the daily or even monthly time resolutions

S. Fatichi (✉) · E. Caporali
Department of Civil and Environmental Engineering,
University of Firenze, Florence, Italy
e-mail: simone.fatichi@ifu.baug.ethz.ch

Present Address:

S. Fatichi
Institute of Environmental Engineering, ETH Zürich,
Wolfgang-Pauli-Str. 15, HIL D 23.2, 8093 Zurich, Switzerland

V. Y. Ivanov
Department of Civil and Environmental Engineering,
University of Michigan, 1351 Beal Avenue,
105 EWRE, Ann Arbor, MI, USA

(Müller-Wohlfeil et al. 2000; Hay et al. 2002; Wilby et al. 2002; Barnett et al. 2004; Wood et al. 2004; Schmidli et al. 2006; Merritt et al. 2006; Leander and Buishand 2007; Burton et al. 2010). A progress in improving spatial resolutions has been achieved with methodologies that combine dynamic downscaling with statistical downscaling, for instance, the quantile-based error correction of Regional Climate Model (RCM) realizations (Quantile Mapping) (Ines and Hansen 2006; Piani et al. 2009; Hurrell and Gleckler 2008; Bárdossy and Pegram 2011), or other empirical statistical methods (Themßl et al. 2011). However, fine temporal resolutions still represent a limitation of recently developed downscaling methodologies (Maraun et al. 2010). This limitation, for example, has direct consequences on the reproduction and prediction of extreme events. An improvement of these skills remains one of the biggest challenges posed to downscaling methodologies (Fowler et al. 2007b; Déqué 2007; Hurrell and Bárdossy 2008; Lenderink and vanMeijgaard 2008; Fowler and Wilby 2010) and represents the missing step to predict the “vital details” of climate change needed by public authorities or engineers (Kerr 2011). Hourly (or shorter) temporal and local (station level) spatial resolutions can be of paramount importance for hydrological, ecological, geomorphological, and agricultural applications. Furthermore, in many environmental applications the two typically downscaled variables, i.e., precipitation and air temperature (Déqué 2007; Vrac and Naveau 2007; Piani et al. 2009; Themßl et al. 2011; Fowler and Wilby 2010; Johnson and Sharma 2011; Groppelli et al. 2011), may not be sufficient for detailed studies of climate change effects, since other meteorological variables also modulate the system response. Finally, the need to account for the uncertainty in climate change predictions, as obtained from a multi-model ensemble, can be also regarded as a fundamental task in downscaling studies. This uncertainty is entirely neglected using a single GCM realization, and partially neglected using the mean or the median of an ensemble (Knutti 2010).

Given the need to find alternative solutions to address the above limitations, this study extends a previously developed stochastic downscaling technique of Fatichi et al. 2011. The overall goal is to provide future climate time series for several hydrometeorological variables that fully address the issue of uncertainty inherent to GCM projections. Specifically, the stochastic downscaling uses a weather generator, the Advanced WEather GENERator (AWE-GEN) to simulate the time series of projected future climate at the station-level and at the hourly time scale. The weather generator has been demonstrated to satisfactorily reproduce a large set of climate variables and statistics over a range of temporal scales, from extremes to low-frequency inter-annual variability

(Fatichi et al. 2011). One of the novelties contributed by Fatichi et al. 2011 was represented by the capability to account for the uncertainty of individual projections by using an ensemble of GCM realizations. However, the methodology only partially addressed this uncertainty by using the mean/median of a GCM ensemble. In this study, the uncertainty of GCM projections is explored further through the generation of an ensemble of time series of meteorological variables, such as precipitation, air temperature, relative humidity, wind speed, and solar radiation.

An ensemble of alternative scenarios of the future is generated by using factors of change corresponding to different probabilities of marginal density functions of factors of change, associated with a given climate change scenario. Specifically, factors of change are sampled from their distributions using Monte Carlo method to entirely account for the probabilistic information obtained with the Bayesian multi-model approach (Tebaldi et al. 2004, 2005; Fatichi et al. 2011). Monte Carlo sampling technique requires certain assumptions about the dependence/independence among the factors of change and such assumptions are developed in this study. The derived factors of change are applied to the statistics inferred from historical observations to re-evaluate the parameters of the weather generator, which is used to obtain alternative climate scenarios.

Several studies expressed certain confidence that a GCM ensemble can provide more reliable projections of climate change or, at least, that the uncertainty is reasonably well captured by the variation among different models (Räisänen 2007; Knutti 2008). However, the notion that model weighting is an improvement in climate change predictions (Lambert and Boer 2001; Tebaldi and Knutti 2007; Reichler and Kim 2008; Pierce et al. 2009), when compared to the use of a single climate model (typically, subjectively selected), or when individual model performances are ignored (i.e., a simple average of model outputs is used) has been recently challenged (Knutti et al. 2010; Weigel et al. 2010; Christensen et al. 2010). The argument has been that while model weighting is promising in principle, the lack of correlation or information on the relation among error characteristics and climate change variables hampers the possibility of obtaining robust weights (Weigel et al. 2010; Giorgi and Coppola 2010); simple averaging might be preferred to avoid another level of uncertainty (Knutti et al. 2010; Christensen et al. 2010). The relative interdependence among models represents a further issue in using model weighting techniques (Masson and Knutti 2011). One of the contributions of this study is a comparison of the methodology that assigns specific weights to different members of a GCM ensemble with a simple average of the ensemble (i.e., equal weighting), representing a more conventional approach to downscaling.

This allows us to evaluate the differences and an added value of multi-model weighting in the final product of the downscaling—an ensemble of alternative climate scenarios.

The presented application focuses on the location of Firenze (Italy), where changes of climate may bring about not only impacts on the natural environment but also on human activities, such as tourism (Berrittella et al. 2006; Amelung et al. 2007), or preservation of important historic-monumental heritage (Lefèvre et al. 2010). This study compares a control scenario characterized by climate over the period of 1962–1992, with three different time periods of future climate: 2000–2009, 2046–2065, and 2081–2100. The first time interval is regarded as a hypothetical “future”, where climate predictions can be simulated according to the presented methodology but observations of the actual climate realization are also available. This time overlap allows one to partially evaluate the reliability of the presented methodology in simulating the expected future. Such an approach cannot be regarded as a full validation in the conventional sense of this term. However, it is important because it represents an assessment of reliability of the presented methodology and can be therefore thought of as an indirect test of numerous assumptions employed by the approach. Furthermore, to the author’s knowledge, this is the first time a downscaling technique is effectively tested in reproducing an observed climate, considering it in a “future-like” mode, as opposed to validation in terms of downscaling/reproducing past climates or through “pseudorealities” (Denis et al. 2002; Vrac et al. 2007; Maraun et al. 2010).

2 Methodology

The stochastic downscaling methodology uses the AWE-GEN (Ivanov et al. 2007; Fatichi et al. 2011) to generate continuous time series of hydroclimatic variables for three time intervals considered as “future”. The three periods are 2000–2009, 2046–2065, and 2081–2100. As a necessary condition of the methodology, all of these time periods are assumed to be stationary. The weather generator is also used to simulate the observed climate, defined as the “control scenario”, or as the “training” period, since the generator parameters are derived using data for this period. The control scenario (CTS) is the thirty-one year long period of 1962 through 1992. Note that the historical period of 2000 through 2009 is regarded as “future” in this study. The motivation is to provide an assessment of reliability of the stochastic downscaling methodology. Given the uncertainty of characterizing climate statistics for a 10 year-period, the comparison is

limited, i.e., it cannot fully evaluate the downscaling methodology. Nonetheless, it provides useful insights on the capabilities of the methodology. For example, the comparison illustrates whether consistent results can be obtained for different aggregation intervals or variables that are not directly downscaled from climate models, e.g., hourly time scales and meteorological variables other than precipitation and air temperature. Note that the time interval between the mid-point years of the training and the first assessment periods (i.e., 1977 and 2005) is 28 years. Such a period is comparable to the time interval of climate change projection for the near-future and the comparison is therefore subject to similar uncertainties and issues.

2.1 Stochastic downscaling

The theoretical basis and procedural steps of the stochastic downscaling methodology are discussed in detail in Fatichi et al. 2011 and only briefly summarized here. Overall, the stochastic downscaling methodology allows one to derive the distributions of factors of change that are calculated as ratios or “delta” differences of climate statistics (Anandhi et al. 2011) for historical and future periods. More specifically, a set of factors of change is computed at the station level to reflect changes in the mean monthly air temperature and several statistics of precipitation (e.g., mean, variance, skewness, frequency of no-precipitation) at different aggregation periods, as a result of comparing historical and predicted climate.

The factors of change derived from a GCM realization can be subsequently applied to a set of statistics of observed climate in order to obtain statistics representative of future climate (Kilsby et al. 2007; Burton et al. 2010; Fatichi et al. 2011). Using these statistical properties, an updated set of AWE-GEN parameters is estimated (Fatichi et al. 2011). As noted previously, each set of AWE-GEN parameters (i.e., a “parameterization”) is calculated assuming climate stationarity for any considered period. The re-parameterized weather generator can be successively used to simulate hourly time series of hydro-climatic variables that are considered to be representative of the predicted climate.

Multi-model realizations of GCM can be also used, which thus can yield an ensemble of sets of factors of change. In this study, realizations from twelve general circulation models are used in all of the analyses (Fig. 1). These models represent a subset of GCMs used in the fourth assessment report (4AR) of the IPCC (Meehl et al. 2007a, b). The realizations correspond to the A1B emission scenario (IPCC 2000). Therefore, the uncertainty related to the plausibility of different emission scenarios is not accounted for in this study.

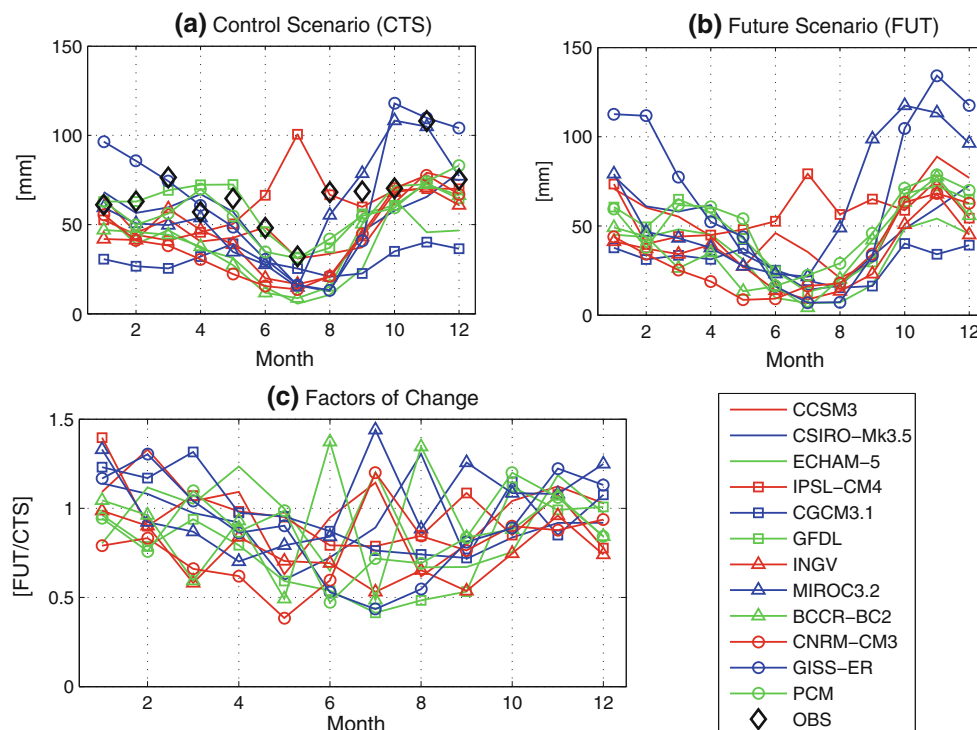


Fig. 1 The time series of total monthly precipitation calculated from observations (OBS) and twelve GCMs: CCSM3, CSIRO-Mk3.5, ECHAM5-MPI-OM, IPSL-CM4, CGCM3.1(T63), GFDL-CM2.1, INGV-SXG, MIROC3.2(medres), BCCR-BC2, CNRM-CM3, GISS-

ER, and PCM for the location of Firenze: **a** Control scenario (CTS), 1962–1992; **b** future scenario (FUT), 2046–2065; **c** product factors of change for monthly precipitation

An ensemble of GCM realizations results in an ensemble of sets of factors of change (Fig. 1), which poses the challenge of including the associated uncertainty in downscaling studies. This source of uncertainty is regarded as one of the principal in climate change studies (Déqué et al. 2005; Räisänen 2007; Knutti 2008; Prein et al. 2011; Hawking and Sutton 2011). The simplest way to proceed is to average the factors of change among different sets, obtaining a single factor for each climate variable/statistic (IPCC 2007). This implies that multi-model information would be retained in the methodology only in a limited fashion: the factors of change are the result of averaging of a model ensemble but their distribution is neglected. Advanced techniques proposed recently take into account the projection information more completely (Giorgi and Mearns 2003; Tebaldi and Knutti 2007). A specific technique used in our previous study (Fatichi et al. 2011) weights the predictions of different members of an ensemble of climate models using a Bayesian approach (Tebaldi et al. 2004, 2005; Smith et al. 2009; Manning et al. 2009). This approach can use either equal weights or weights computed according to specific criteria, for instance, convergence among model realizations and model bias with respect to the historical climate (Tebaldi et al. 2004, 2005). Any of such possible weighting methods

produces probability density function (PDF) for each factor of change (e.g., mean monthly temperature, mean and variance of precipitation over 24-hour period, etc.) (Tebaldi et al. 2005; Fatichi 2010).

2.2 Sampling of factors of change

A significant challenge is posed by the need to keep probabilistic information on future changes in the final output of a stochastic downscaling procedure, such as hourly time series of meteorological variables. In Fatichi et al. 2011, AWE-GEN was used to generate the time series of predicted *mean/median* future climate, using a single set of weather generator parameters corresponding to the means/medians of the PDFs of factors of change. Such an approach produced a single, *most probable* future climate (Fatichi et al. 2011), yet neglecting most of information contained in the PDFs.

Transferring the complete uncertainty contained in the PDFs of factors of change into generated meteorological time series can be regarded as the ultimate step in a downscaling methodology, allowing one to account for a heterogeneous nature of climate predictions produced by different models. This step calls for a Monte Carlo simulation approach (e.g., Robert and Casella 2010) that poses

several challenges. Firstly, a Monte Carlo application requires assumptions about the dependence/independence of the factors of change. Secondly, a numerical methodology must be used because a joint probability density function that combines all of the factors of change can not be defined in an analytical form; also the marginal distributions of factors of change can only be derived empirically through a Monte Carlo Markov Chain (MCMC) approach (Tebaldi et al. 2004, 2005; Fatichi 2010, Fatichi et al. 2011). Recently, joint distributions of the factors of change for average seasonal temperature and average seasonal precipitation were obtained numerically (Tebaldi and Sansó 2009) but are still too simplified to be suitable for the stochastic downscaling with AWE-GEN.

A Monte Carlo simulation implies that random factors of change must be generated according to their distributions. In total, the stochastic downscaling technique derives 170 PDFs of factors of change from an ensemble of climate models (Fatichi et al. 2011). These include 12 PDFs for the monthly air temperature, T_{mon} , (i.e., one for each month), 12×4 PDFs for each precipitation statistics, which are four in total (i.e., the factors of change are computed on a monthly basis for the mean $E_{P_r}(h)$, variance $VAR_{P_r}(h)$, frequency of no-precipitation, $\Phi_{P_r}(h)$, and skewness, $SKE_{P_r}(h)$, at different aggregation periods, specifically, $h = 24, 48, 72,$ and 96 h), and 2 PDFs for the coefficient of variation and the skewness of the annual precipitation process, $\overline{Pr_{yr}}$ (see Fatichi et al. 2011). One may note that $12 + 4 \times 12 \times 4 + 2 = 206$, however, the product factors of change for mean precipitation, $E_{P_r}(h)$, are the same regardless of the aggregation period because of the linearity of the mean operator. Consequently, only 12 PDFs of factors of change for mean precipitation, E_{P_r} , are generated and the random selection is constrained to 170 PDFs.

2.3 Cross-correlation among factors of change

The correlation among the factors of change is intrinsic to the methodology because the PDFs of the factors of change are obtained using GCM realizations that produce climate variables and statistics that are physically correlated. However, an exact cross-correlation among the factors of change is unknown and must be assumed. This poses a further challenge in transferring the uncertainty from the marginal PDFs of the factors of change to the time series sought to be generated by the downscaling procedure. The simplest way to approach the problem is to assume a complete independence among some of the estimated factors of change. For instance, although some degree of correlation is expected between future changes in precipitation and air temperature (Tebaldi and Sansó 2009), the GCM-derived changes of these two variables can be

assumed to be fairly independent. However, statistical independence would be difficult to justify for changes of the same variable but in different months, e.g., delta-changes of air temperature in consecutive months cannot be assumed to be entirely independent. The same consideration applies to changes of the same variable at different aggregation periods, e.g., changes in the variance of precipitation at 24 and 48-hour intervals are undoubtedly strongly correlated. Consequently, some of the variables can be hypothesized to have a strong correlation. Such a hypothesis is probably acceptable for the factors of change of the same variable at different months and aggregation periods.

It is impossible to identify a theoretical solution for the issue of cross-correlation among the factors of change, since it is impossible to find the complete structure of a multivariate PDF only having the marginal PDFs. Data do not exist and will unlikely come to existence to quantify the cross-correlations among different factors of change, which are thus highly uncertain. A pragmatismal solution must be adopted. Specifically, in this study the 170 factors of change are reduced to 7 independent groups. The factors of change are assumed to be entirely uncorrelated among the groups. Within each group, a complete dependence among the factors of change is assumed. The group compositions are described in Table 1. As seen, the factors of change among different precipitation and air temperature statistics are considered to be completely independent. The factors of change for different months and aggregation

Table 1 The partition of factors of change of the downscaling procedure into groups

Group	Variable	Number of factors of change
1	T_{mon}	12 (monthly)
2	$VAR_{P_r}(h)$	12×4 (monthly and $h = 24, 48, 72, 96$ h)
3	$\Phi_{P_r}(h)$	12×4 (monthly and $h = 24, 48, 72, 96$ h)
4	$SKE_{P_r}(h)$	12×4 (monthly and $h = 24, 48, 72, 96$ h)
5	$E_{P_r}(h)$	12 (monthly)
6	C_v of $\overline{Pr_{yr}}$	1
7	Skewness of $\overline{Pr_{yr}}$	1

Within each group, the factors of change are assumed to be perfectly correlated, i.e., the coefficient of correlation is equal to one. Among the groups, the factors of change are assumed to be independent, i.e., their cross correlations are equal to zero. The term T_{mon} represents the monthly air temperature, $VAR_{P_r}(h)$ is the precipitation variance, $\Phi_{P_r}(h)$ is the frequency of no-precipitation, $SKE_{P_r}(h)$ is the precipitation skewness, $E_{P_r}(h)$ is the precipitation mean, $\overline{Pr_{yr}}$ is the annual precipitation, C_v is the coefficient of variation

periods but the same variable are assumed to be perfectly correlated, i.e., the changes of a statistic at different months and aggregation periods have cross-correlations equal to one. For instance, a change in the precipitation variance for a 24-hour aggregation period is fully correlated with the change for a 72 h period.

2.4 Generation of an ensemble of future climate time series

Given the above assumptions of cross correlations among the factors of change, each Monte Carlo iteration consists in generation of only 7 independent random numbers (specifically, cumulative probabilities of PDFs), one for each group. The generated cumulative probabilities, p_i , $i = 1, \dots, 7$, are used to estimate the factors of change for each PDF of the corresponding group (see Table 1). For instance, in a single Monte Carlo iteration, a random cumulative probability p_1 is generated to estimate the additive factor of change for T_{mon} for each month. A random cumulative probability p_2 is generated to estimate the product factors of change for $VAR_{p_r}(h)$ for each month and at the four aggregation intervals: 24, 48, 72, and 96 h. Similar considerations can be extended to the other remaining groups (3 through 7) with p_3, \dots, p_7 .

Note that the same cumulative probability does not necessarily imply the same factor of change, because the latter depends on the shape of the marginal PDF. The PDFs of the factors of change are generally different within the same group of PDFs and across groups. Given the numerical representation of these distributions, further details on calculation of these PDFs are warranted and provided in the following.

In total, one thousand sample values are used for each factor of change to define a PDF and its integral, i.e., the cumulative distribution function (CDF). The samples are the result of the Monte Carlo Markov Chain (MCMC) method, as described in Tebaldi et al. 2005 and Fatichi 2010. Specifically, a Gibbs sampler is used to simulate the joint posterior distribution of the multi-model ensemble by iteration on a sequence of full conditional distributions. Empirical probabilities are assigned to each sample with a plotting position method (Cunnane 1978). Once a random number, p , distributed uniformly between 0 and 1 has been generated in the Monte Carlo procedure, a linear interpolation of the CDF is used to find the exact value of the factor of change corresponding to the cumulative probability p .

Following the described procedure of a single iteration for a single probability p , \bar{N} Monte Carlo iterations, equal to the number of desired alternative ensemble series, are carried out, each time generating seven random

probabilities, p_i , $i = 1, \dots, 7$, and thus yielding 170 factors of change (correlated as described previously). Each of \bar{N} sets of factors of change is applied to the climate statistics inferred from observed data in order to obtain modified statistics representative of a possible climate for a future period. The procedure is exactly equivalent to the use of a *mean/median* set of factors of change described in Fatichi et al. 2011. However, in Monte Carlo sampling the process is iterated \bar{N} times, fully exploring the probabilistic information contained in the PDFs of factors of change. Once all of the statistical properties are calculated for \bar{N} representations of a future climate period, \bar{N} sets of AWE-GEN parameters are estimated.

2.5 Ensemble types

Several approaches for computing an ensemble of parameterizations are considered in this study with the overarching goal to represent different probabilistic expressions of future climate. The parameterizations are calculated either as a result of processing PDFs of factors of change (i.e., an infinite number of possible parameterizations) or by using a single set of factors of change.

Specifically, Bayesian weighted averaging (BWA) approach combines factors of change of GCM members according to the criteria of convergence among model realizations and model bias with respect to a historical climate (Tebaldi et al. 2004, 2005; Fatichi et al. 2011). The methodology leads to different weights for the factors of change obtained from different GCMs. Conversely, equal weights are introduced through Bayesian simple averaging (BSA). Both of the methods result in the PDFs of factors of change (Fig. 2). A single set of factors of change is obtained through simple averaging (SA) of factors of change of a GCM ensemble. The SA case represents the most typical downscaling application. Note that while the BSA approach is introduced here as one of the possible alternatives, it is not discussed in the results sections.

In the case of the Bayesian approach, since the factors of change are randomly combined for each Monte Carlo iteration, \bar{N} generated parameterizations generally differ from each other in terms of characteristics such as the mean precipitation, the mean air temperature, the inter-annual variability of precipitation, the internal structure of precipitation, etc. As \bar{N} increases, the multiple combinations of the factors of change allow one to explore a wider set of possible future scenarios. Therefore, the effects of assumptions made with regards to cross-correlation of the factors of change tend to become less important. Nonetheless, the computational time required to take the full advantage of the methodology grows with \bar{N} considerably, making it less suitable for typical modeling applications.

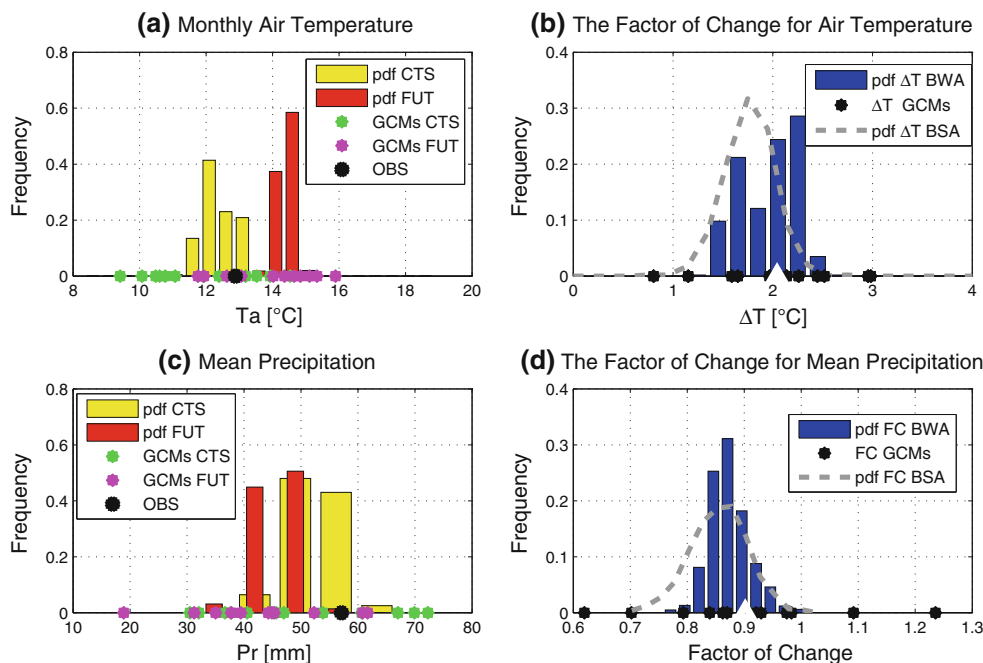


Fig. 2 Observations and probability density functions (PDFs) obtained for two climate variables using a multi-GCM ensemble for the location of Firenze, the month of April. **a** The PDF of mean April temperature for CTS (1962–1992) (yellow bars) and FUT (2046–2065) (red bars) scenarios. Also shown are the observations (OBS) and results from the individual models for the CTS (green dots) and FUT (magenta dots) scenarios. **b** The PDF of the additive factor of change for air temperature obtained with a Bayesian weighted (BWA) multi-model ensemble (blue bars) and the PDF obtained using equal weights (BSA) approach (gray dashed line). Also shown are the predictions by the individual models (black dots) and the simple average (SA) of all models (white triangle). **c** The PDF obtained of mean April precipitation for the CTS (yellow bars) and FUT (red bars) scenarios. Also shown are the observations (OBS) and results from individual models for the CTS (magenta dots) and FUT

(green dots) scenarios. **d** The PDF of the product factor of change for precipitation obtained with a Bayesian weighted (BWA) multi-model ensemble (blue bars) and the PDF obtained using equal weights (BSA) approach (gray dashed line). Also shown are the predictions by the individual models (black dots) and the simple average (SA) of all models (white triangle). Note that the distribution obtained using equal weights (BSA) has a different mean from the simple average of factor of changes (SA) because two parameters affect the outcome of the BSA weighting: θ (the inflation–deflation parameter that represents the relative weight of future realizations of GCMs compared to the control scenario realizations) and β (the correlation parameter that represents a possible dependence between GCM simulations in the control scenario and future conditions) that are determined by the MCMC procedure (Tebaldi et al. 2005; Fatichi 2010)

An ensemble size of $\bar{N} = 50$ was used in this study as a representative number allowing one to demonstrate the range of uncertainty in the factors of change without excessively large computational requirements. Specifically, fifty ensemble parameterizations were computed with the BWA approach and used for the generation of fifty 30-year long time series for each of the three time windows: 2000 through 2009, 2046 through 2065, and 2081 through 2100. In the SA case, only a single set of factors of change can be generated for each period of interest. Fifty time series were generated for each of the tree time windows by using the same parameterization of the weather generator but different random seeds at the beginning of each generation simulation. Note that the fifty series only address the intrinsic stochastic variability of the climate process

Additional three 30-year long series were generated to represent a possible form of the “likeliest” expression of future climates for each of the considered time windows. Specifically, the corresponding AWE-GEN parameterizations

were obtained by using the medians of the PDFs of factors of change obtained with the BWA approach (i.e., the series do not represent the medians of ensembles for the respective periods). The same approach was used in Fatichi et al. 2011.

Finally, one hundred 30-year long series representing the control scenario (CTS), i.e., representative of historical climate over the period of 1962 through 1992, were simulated using the AWE-GEN parameterization derived using observations for this period. The generated series allow us to explore the stochastic variability of hydrometeorological variables. Stochastic realizations of 30-year long time-series are generally insufficient to represent such variables as precipitation and thus an ensemble is preferred to fully reflect the process of stochasticity.

Theoretically, a stochastic ensemble (of, say, 30-year long series) could be generated for each possible representation of future climate, expressed with a given AWE-GEN parameterization. For example, a stochastic ensemble can be generated for each of the $\bar{N} = 50$ climate

alternatives, for each future time window. This would allow one to simultaneously consider both the uncertainty of climate change projections and the stochastic variability within the assumed stationary climate. Given the computational burden implied by such a large number of simulations, the stochastic variability of a given climate representation is only explored for (a) the control scenario climate and (b) the SA case. While limited, inferences with regards to the other types of climate projections are still meaningful: the stochastic variability is partly reflected in 30-year long series and an ensemble of projected climates for a given period is expected to represent most of the stochastic variability (Deser et al. 2012). For example, ensemble members corresponding to the same probabilities of the factors of change CDF will correspond to “fairly similar” climates with different stochastic trajectories.

3 Data

The reference climate used in this analysis is that of Firenze (11.25E, 43.76N; elevation 50.1 m a.s.l., Italy), where observations were available as a combination of different datasets, as described in the following. Hourly air temperature, wind speed, relative humidity, and atmospheric pressure for the period of 1962 through 2010 were obtained for the Firenze Peretola station from the National Climatic Data Center (NCDC) (Peterson and Vose 1997). The dataset of Firenze Peretola lacks precipitation series and was replaced with observations obtained for the Firenze Ximeniano station. The station is a part of the Tuscany region precipitation network and is located about 5.5 km from Firenze Peretola. Data were available for the periods of 1962–1992 and 2000–2009. The small distance between the two stations does not appreciably affect the results of this study. Finally, the shortwave radiation and cloudiness parameters of the weather generator were estimated from the data for another station, Firenze Università (about 2.1 km distant from Firenze Ximeniano), available for the period of 2000 through 2009 (Fatichi et al. 2010). Since no information was available for the period of 1962 through 1992, the 2000–2009 parametrizations for shortwave radiation and cloudiness, were also used over the former period to make feasible weather generator simulations.

Model realizations for twelve GCMs were obtained from the dataset compiled in the World Climate Research Programme’s (WCRP’s), Coupled Model Intercomparison Project, Phase 3 (CMIP3) (Meehl et al. 2007a). Specifically, climate realizations for the following models were used in this work: *CCSM3*, *CSIRO-Mk3.5*, *ECHAM5-MPIOM*, *IPSL-CM4*, *CGCM3.1(T63)*, *GFDL-CM2.1*, *INGV-SXG*, *MIROC3.2(medres)*, *BCCR-BC2*, *CNRM-CM3*, *GISS-ER*, and *PCM*. The selection of GCMs was based on

similar criteria used by Fatichi et al. 2011. Data for air temperature and precipitation were available for all of the models at the daily time scale over the periods of 2046–2065 and 2081–2100. Using the same reasoning as outlined in Fatichi et al. 2011, this study used outputs of GCMs for a grid cell that contained the location of Firenze.

Since not all of the models had outputs for the “validation” period of 2000–2009, the factors of change for this period were estimated using the methodology of interpolating transient factors of change presented by Burton et al. 2010. Specifically, the factors of change for each GCM for any given year (e.g., 2005) were obtained through a linear interpolation of the factors of change for the period of 2046 through 2065 and the “factors of change” for the period of 1962 through 1992 (all equal to unity or zero). In comparison to Burton et al. 2010, a single set of factors of change was used for the period of 2000 through 2009, which was assumed to be stationary. Specifically, the interpolated factors of change for the year 2005 were used. The factors of change obtained for all of the 12 GCMs were successively weighted with the Bayesian approach to produce probabilistic information of the change for that time period in a similar fashion, as for the future time periods (e.g., Fig. 2).

4 Results

A comparison between the observations and weather generator simulation for the control scenario and the “validation” (i.e., 2000–2009) periods are illustrated first. Such a comparison highlights the capability of AWE-GEN in reproducing the already observed climate and provides a first assessment of reliability of the stochastic downscaling methodology. An ensemble of simulated climates for the periods of 2046 through 2065, and 2081 through 2100 are also illustrated and discussed subsequently.

4.1 Precipitation

Mean monthly precipitation of the control scenario is exactly reproduced by AWE-GEN, when the one hundred of 30-year long series are averaged (Fig. 3a). If only a single 30-year climate trajectory is used, the differences of about 10–15 mm month⁻¹ can be observed, as demonstrated by the ranges between the 5th and 95th percentiles of monthly precipitation, derived using all of the 100 ensemble members (Fig. 3a). Defining the possible stochastic variability for a single 30-year realization of climate is important in order to properly frame a discussion of precipitation changes in future. As seen in the figure, the simulated monthly precipitation for the “validation” period of 2000–2009 is relatively unchanged, when compared to

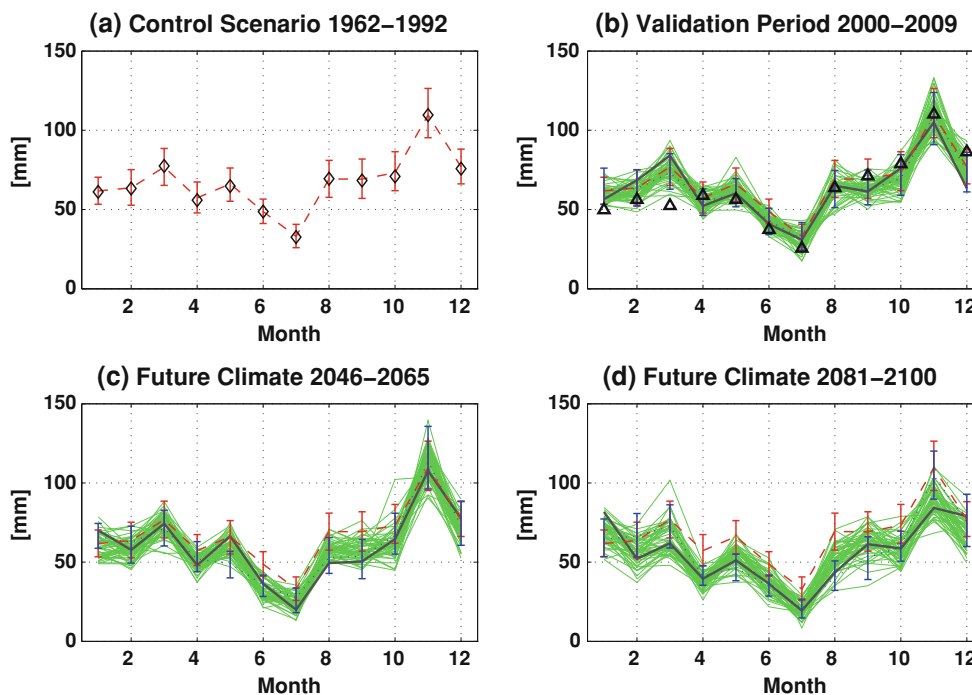


Fig. 3 Mean monthly precipitation observed and simulated with the weather generator for different climate periods **a** 1962–1992, **b** 2000–2009, **c** 2046–2065, and **d** 2081–2100. The *diamonds* represent the observed values for the period of 1962–1992 (subplot **a**), and the *triangles* represent the observed values for the period of 2000–2009 (subplot **b**), the *dashed line* is the mean of the ensemble of AWE-GEN generated climate trajectories for the control scenario, the

vertical bars represent the 5th and 95th percentiles (subplots **a**, **b**, **c**, and **d**), the *solid gray lines* represent the result obtained using the medians of the factors of change PDFs (subplots **b**, **c**, and **d**). The thin green lines represent the ensemble of climate realizations obtained with the BWA approach. The *blue dotted lines* and *blue bars* are the results of the SA simulation approach (subplots **b**, **c**, and **d**)

the control scenario (Fig. 3b). The trajectory obtained using the medians of the PDFs of the factors of change differs somewhat from the reference climate (CTS) but is always within the 5–95th percentile range of stochastic variation. The range of monthly precipitation simulated using the factors of change from the SA approach is also very similar to the uncertainty of stochastic simulations for the control scenario, thus entailing a negligible change. When an entire ensemble of possible realizations is considered, the differences between the predicted climate and the stochastic ensemble of the CTS are observed in the months of March, August, and September. In these months several ensemble members exhibit a decrease in precipitation outside of the 5–95th percentile range of the historical climate. When actual observations are considered for the period of 2000–2009, one can see that these are well within the range of variability of the BWA simulated climate for most of the months, with the exception of January and March. For these months, the observed precipitation is significantly less than possible for the period of 1962–1992. This is only partially captured by the simulated climate (Fig. 3b) for March. Despite this difference, the relatively unchanged mean precipitation regime confirmed by both the simulated climate and the observations

corroborates the stochastic downscaling methodology for this climatic property.

A relative change in the precipitation regime is more appreciable when the future period of 2046 through 2065 is analyzed. While the possible trajectories of future climate show a fair amount of uncertainty and do not exclude a “zero-change” scenario, most of the ensemble members and the median show a reduction in precipitation. This is especially pronounced during the summer-fall months (June to September), where more than a half of the simulation members are below the lower uncertainty bounds of precipitation of the control scenario (Fig. 3c). This reduction during spring-summer-fall months is further exacerbated in the far future, during the period of 2081–2100, where majority of the members of the ensemble show lower precipitation (Fig. 3d). Future simulations obtained in the SA case predict similar patterns of change with more pronounced differences in February, March and November during the period of 2081–2100. The uncertainty of stochastic realizations of the SA case overlaps with the multiple simulated scenarios of the BWA approach, although, as expected, tends to be smaller.

Note that the relative uncertainty of the simulated future climates does not change significantly for different periods,

i.e., the range of the BWA ensemble is approximately the same for different periods. This is likely due to the fact that uncertainty is already relatively high in the “validation” period, because of a fairly poor capacity of GCMs to represent historical records. The predicted evolution of the precipitation regime for Firenze implies a change from the simulated annual total of 802 mm year^{-1} (or 796 mm year^{-1} based on observed data) in the control scenario to 764 mm year^{-1} (or 746 mm year^{-1} based on observations) for the period of 2000–2009, to 722 mm year^{-1} for the period of 2046–2065, and as low as 669 mm year^{-1} for the period of 2081 through 2100. The values refer to the simulations with the median factors of change. This represents a -17% change of annual precipitation from the control scenario by the end of the twenty-first century, with a sharper decrease after the year of 2050. The change is mainly concentrated during summer months in the first half of the century and “spreads” to earlier and later months afterwards.

The nature of these changes can be further observed by inspecting the survival functions of hourly precipitation in Fig. 4. AWE-GEN reproduces the entire distribution of precipitation very well in the control scenario, with only marginal differences within the uncertainty bounds for very low exceedance probabilities (Fig. 4a). For the “validation” period of 2000–2009, an increase in the probability of

occurrence of intense precipitation, even outside the uncertainty range, is detectable in the observations and only in some of the most extreme members of the simulated ensemble. This highlights the importance of accounting for the uncertainty in future climate simulations as well as using an ensemble of stochastic trajectories. Using a particular realization obtained as the median climate (gray solid line) would have led to a significantly distorted representation of future intense precipitation (Fig. 4b). Survival functions obtained in the SA case for the period of 2000–2009 are essentially identical to the control scenario. The survival functions of precipitation for the periods of 2046–2065 and 2081–2100 confirm the general tendency to a reduction in precipitation. However, as inferred for the latter period, the reduction in precipitation will be accompanied by an increase of rainfall intensity at low probabilities, as indicated by the different curvatures of lines corresponding to the control scenario and future climate (Fig. 4c, d). While the reduction in precipitation is also confirmed by the SA case, the inferred increase of rainfall intensities is not as pronounced.

The return periods for extreme precipitation for 24-hour aggregation period are shown in Fig. 5. The weather generator reproduces rainfall extremes satisfactorily in the control scenario (Fig. 5a). There is no projected change for

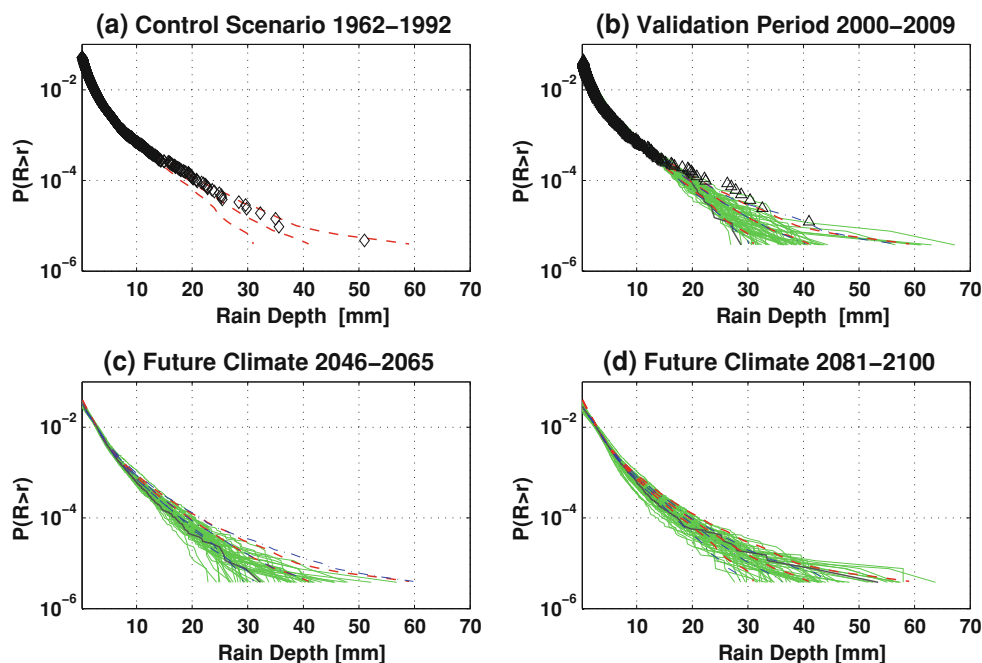


Fig. 4 One hour precipitation survival function from observed data and simulated with the weather generator for different climate periods **a** 1962–1992, **b** 2000–2009, **c** 2046–2065, and **d** 2081–2100. The *diamonds* represent the observed values for the period of 1962–1992 (subplot **a**), and the *triangles* represent the observed values for the period of 2000–2009 (subplot **b**), the *red dashed lines* are the mean and the 5th and 95th percentiles of the ensemble of generated climate

trajectories for the control scenario (subplots **a**, **b**, **c**, and **d**), the *solid gray lines* represent the result obtained using the medians of the factors of change PDFs (subplots **b**, **c**, and **d**). The *thin green lines* represent the ensemble of climate realizations obtained with the BWA approach. The *blue dash-dotted lines* are the results of the SA simulation approach (subplots **b**, **c**, and **d**)

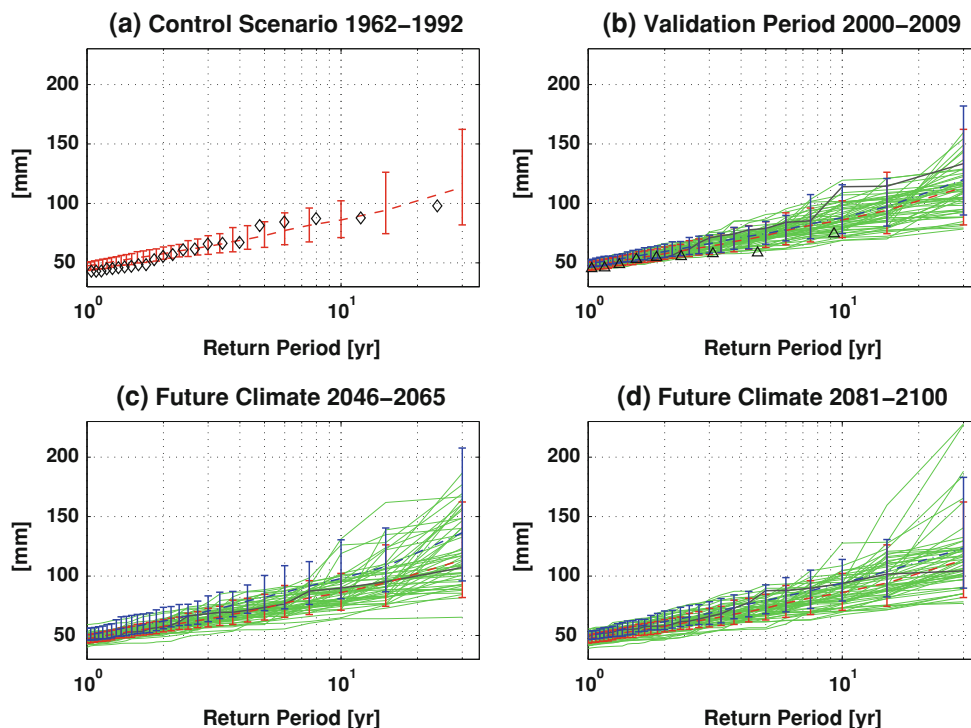


Fig. 5 Extreme precipitation for 24-hour aggregation period from observed data and simulated with the weather generator for different climate periods **a** 1962–1992, **b** 2000–2009, **c** 2046–2065, and **d** 2081–2100. The *diamonds* represent the observed values for the period of 1962–1992 (subplot **a**), and the *triangles* represent the observed values for the period of 2000–2009 (subplot **b**), the *red dashed line* is the mean of the ensemble of generated climate

trajectories for the control scenario, the *red vertical bars* represent the 5th and 95th percentiles (subplots **a**, **b**, **c**, and **d**), the *solid gray lines* represent the result obtained using the medians of the factors of change PDFs (subplots **b**, **c**, and **d**). The *thin green lines* represent the ensemble of climate realizations obtained with the BWA approach. The *blue dash-dotted lines* and *blue bars* are the results of the SA simulation approach (subplots **b**, **c**, and **d**)

the “validation” period since the uncertainty of the BWA ensemble is well within the 5 to 95 percentile bounds of the control scenario climate. The reduction of 24-hour extreme rainfall that appears to be present in the observations can be also explained by the uncertainty of determining precipitation extremes using short observational records (Fig. 5b). It is also important to note that if a single simulation is used, for instance, corresponding to the medians of PDFs of factors of change, this would have led to an erroneous conclusion. In order to make a more certain statement with regards to future extreme events, it is very important to generate an ensemble of realizations that can concurrently capture the uncertainty of climate change projections and inherent stochastic variability (Fig. 5b). In particular, the stochastic variability appears to be dominant for the assessment period of 2000–2009, as testified by simulations obtained with the SA approach.

The projected change of the 24-hour extreme precipitation for the other future periods (Fig. 5c, d) is dominated by uncertainty, however, for most of the BWA ensemble members this uncertainty is still bounded by the variability of stochastic realizations. The future simulations with the SA approach show a more evident increase of 24-hour

extreme precipitation, as compared to the control scenario, regardless of the large stochastic uncertainty. However, the SA bounds still do not include some of the most extreme BWA ensemble realizations.

This large range of projections is not surprising, given the difficulty of transferring climate model information to the reproduction of extreme events and to short observation/simulation periods. Nonetheless, we believe that information produced by this analysis is useful. Even though the uncertainty is large (see the range of ensemble members in Fig. 5d), it provides an approximate range of variability and trends that have a physical basis of changes simulated by climate models, preserved by the weather generator. Note that very intense precipitation events (>150 mm) with return periods above 15 years are simulated as possible (although with low probabilities, i.e., only few ensemble members) only for the 2081–2100 period but not for 2000–2009.

4.2 Air temperature

The mean monthly temperature is reproduced with a high accuracy by the weather generator for the control scenario

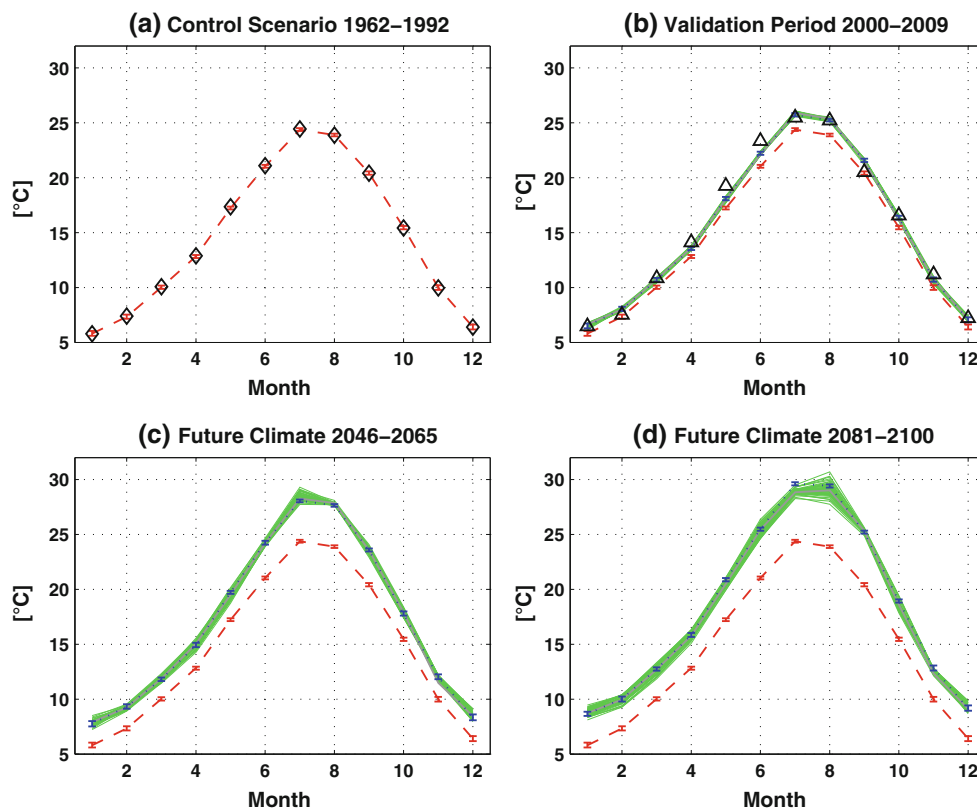


Fig. 6 Average monthly air temperature from the observed data and simulated with the weather generator for different climate periods **a** 1962–1992, **b** 2000–2009, **c** 2046–2065, and **d** 2081–2100. The *diamonds* represent the observed values for the period of 1962–1992 (subplot **a**), and the *triangles* represent the observed values for the period of 2000–2009 (subplot **b**), the *dashed line* is the mean of the ensemble of generated climate trajectories for the control scenario,

the vertical bars represent the 5th and 95th percentiles (subplots **a**, **b**, **c**, and **d**), the *solid gray lines* represent the result obtained using the medians of the factors of change PDFs (subplots **b**, **c**, and **d**). The *thin green lines* represent the ensemble of climate realizations obtained with the BWA approach. The *blue dotted lines* and *blue bars* are the results of the SA simulation approach (subplots **b**, **c**, and **d**)

(Fig. 6a). Contrary to precipitation, the variability introduced by considering an ensemble of one hundred, 30-year long stochastic trajectories of air temperature is almost negligible. The standard deviations of 30-year mean monthly temperatures are around $0.03\text{ }^{\circ}\text{C}$. An annual average increase of $0.92\text{ }^{\circ}\text{C}$ with respect to the control scenario is projected for the “validation” period of 2000–2009, with a larger warming during the summer months (Fig. 6b). This projection agrees very well with the observed change of $1.05\text{ }^{\circ}\text{C}$, providing a strong support to the reliability of both climate predictions and the down-scaling methodology of air temperature. Note that the changes are predicted very well for most months with only a slight underestimation of warming in May and June and a slight overestimation in September. The mean air temperature is projected to increase in future climate conditions for the periods of 2046 through 2065 and 2081 through 2100 by 2.53 and $3.45\text{ }^{\circ}\text{C}$, respectively, as compared to the control scenario (Fig. 6c, d). Note the inferred deceleration of warming for Firenze in the second half of the twenty-first century. Fig. 6 also illustrates how the uncertainty of

the BWA ensemble (referred to here as the ensemble range) grows with time. However, it is not particularly high even for the period of 2081–2100, underlying how climate model predictions tend to be in a general agreement with respect to air temperature changes. The uncertainty is also unevenly distributed throughout the year, with summer months exhibiting the largest range of variability ($\approx 1\text{ }^{\circ}\text{C}$). Future mean monthly temperatures simulated with the SA approach for the period 2081–2100 are always close to the BWA ensemble median or slightly higher (by $\sim 0.2\text{--}0.5\text{ }^{\circ}\text{C}$). The stochastic variability of the SA simulations is practically negligible.

Analogous considerations can be made with respect to the daily maximum, and minimum air temperatures (not shown). The predicted positive changes of maximum and minimum temperatures are uniform: 0.92 , 2.59 , and 3.48 for maximum, and 0.95 , 2.51 , and $3.46\text{ }^{\circ}\text{C}$ for minimum temperatures for the “validation”, 2046–2065, and 2081–2100 periods, respectively. To some extent, such a uniform pattern of changes is corroborated by the fairly similar changes of daily maximum and minimum

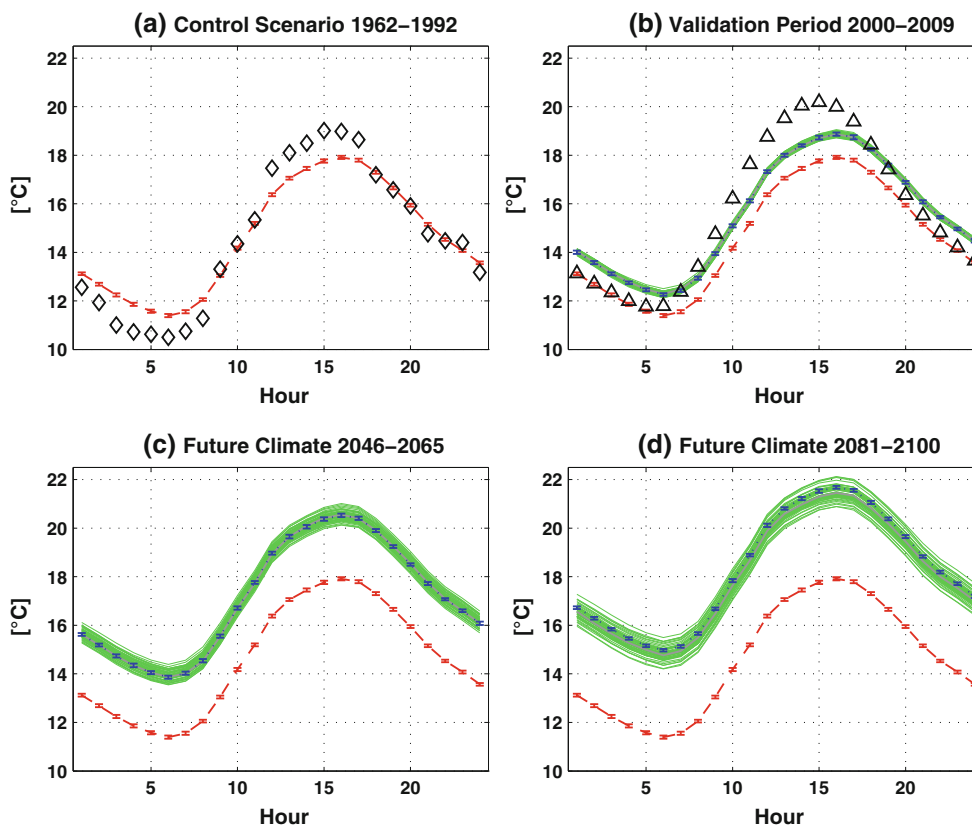


Fig. 7 Mean daily cycle of air temperature from the observed data and simulated with the weather generator for different climate periods **a** 1962–1992, **b** 2000–2009, **c** 2046–2065, and **d** 2081–2100. The *diamonds* represent the observed values for the period of 1962–1992 (subplot **a**), and the *triangles* represent the observed values for the period of 2000–2009 (subplot **b**), the *dashed line* is the mean of the ensemble of generated climate trajectories for the control scenario,

the *vertical bars* represent the 5th and 95th percentiles (subplots **a**, **b**, **c**, and **d**), the *solid gray lines* represent the result obtained using the medians of the factors of change PDFs (subplots **b**, **c**, and **d**). The *thin green lines* represent the ensemble of climate realizations obtained with the BWA approach. The *blue dotted lines* and *blue bars* are the results of the SA simulation approach (subplots **b**, **c**, and **d**)

temperatures estimated from observations for the control scenario and the validation period: 1.15 and 1.06 °C, respectively. A clear seasonal pattern, consistent with the changes simulated for the mean temperature, i.e., a stronger warming during summer, is similarly reproduced.

The diurnal cycle of mean air temperature is simulated realistically by AWE-GEN in the control scenario, even though non-negligible differences of 0.5–1 °C during early morning and midday hours can be observed (Fig. 7a). These differences are due to a poor performance of the weather generator in reproducing the exact daily cycle for the location of Firenze Peretola, most probably due to the interpolation of three-hour observation intervals in the NCDC record. This precludes a direct comparison in terms of absolute hourly values for the “validation” period, since the errors are of the same magnitude as the expected change. The simulated and observed daily cycles of temperature for the period of 2000–2009 show that the overall direction and magnitude of the change are fairly well captured by the stochastic downscaling. The distribution of

the warming signal between daylight (6–18) and night (0–6 and 19–23) hours is however not well captured (Fig. 7b). The observed warming of 1.48 °C (1962–1992 vs. 2000–2009) during the daylight hours is larger than that during night hours, 0.75 °C. The simulated warming for different parts of the day is only slightly different, i.e., the changes during day-light and night-time hours are 0.94 and 0.91 °C, respectively. The parameterization of the weather generator is currently unable to reflect differences in warming across the daily cycle. Note however, that the factors of change for air temperature are calculated only at the monthly scale. This shortcoming points to the need of estimating the factors of change from climate model realizations at the hourly scale, in order to better describe the intra-daily variability. Presently, the solution of this issue is only constrained by current practices of GCM data archiving and their availability: all climate models can produce information at such fine time scales and it can be used by stochastic downscaling methodologies, such as the one employed in this study.

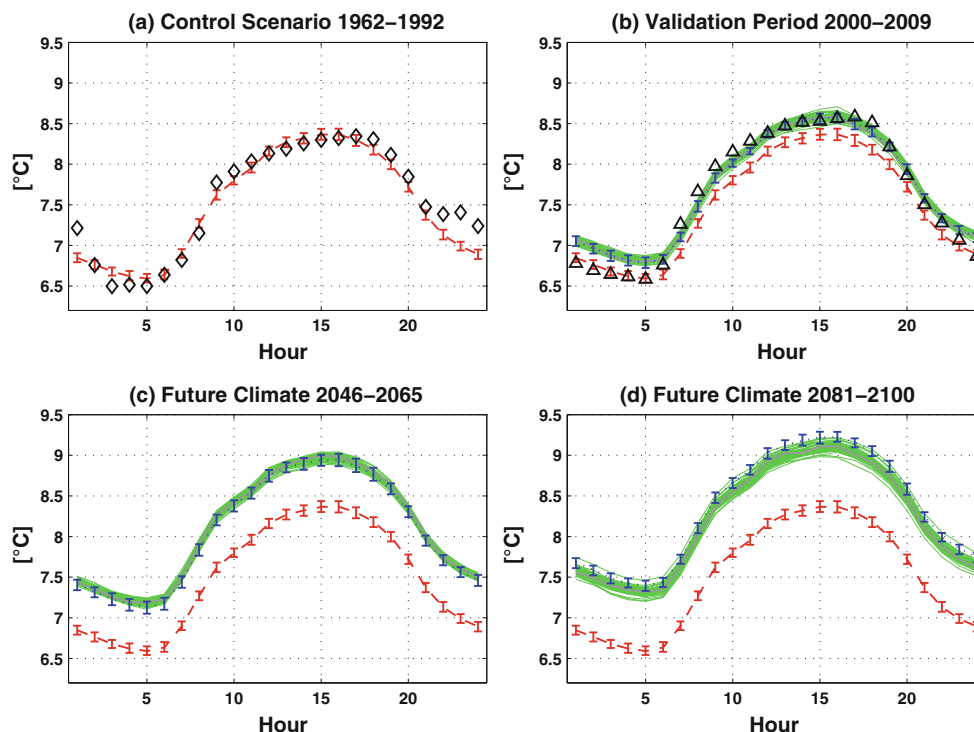


Fig. 8 The diurnal cycle of average standard deviation of hourly air temperature from the observed data and simulated with the weather generator for different climate periods **a** 1962–1992, **b** 2000–2009, **c** 2046–2065, and **d** 2081–2100. The *diamonds* represent the observed values for the period of 1962–1992 (subplot **a**), and the *triangles* represent the observed values for the period of 2000–2009 (subplot **b**), the *dashed line* is the mean of the ensemble of generated climate

trajectories for the control scenario, the *vertical bars* represent the 5th and 95th percentiles (subplots **a**, **b**, **c**, and **d**), the *solid gray lines* represent the result obtained using the medians of the factors of change PDFs (subplots **b**, **c**, and **d**). The *thin green lines* represent the ensemble of climate realizations obtained with the BWA approach. The *blue dotted lines* and *blue bars* are the results of the SA simulation approach (subplots **b**, **c**, and **d**)

The simulated warming for the periods of 2046–2065 and 2081–2100 is fairly similar across all hours of the day and coincides with the mean annual warming (Fig. 7c, d). It can be also noticed that the BWA uncertainty of simulated future temperature tends to increase significantly for scenarios that are more distant in the future.

The simulated and observed standard deviations of the daily cycle of air temperature are shown in Fig. 8a. AWE-GEN is able to reproduce the diurnal distribution of standard deviation of air temperature in the control scenario very well. The observed and simulated delta changes of standard deviations of the daily cycle between the control scenario and the 2000–2009 period are very similar on average, $+0.11$ and $+0.16$ °C respectively, with data for most of the hours well within the BWA uncertainty bounds. This is a rather surprising result since the mean monthly temperature is the only property for which the factors of change are computed. This further corroborates the stochastic downscaling methodology that provides realistic changes for the second order statistics, which are only a result of the weather generator simulation, increasing confidence in the reliability of internal assumptions. The standard deviation of the daily cycle of air temperature is

simulated to further increase in the future periods of 2046–2065 and 2081–2100. Most of the change is projected to occur between the 2000–2009 and 2046–2065 periods (Fig. 8c, d). The uncertainty of changes of standard deviation appears to be smaller than that for the daily cycle of mean air temperature but it is hard to assert whether this occurs by chance or is a consistent prediction. The simulated standard deviations of temperature of the SA approach overlap with the median for the 2000–2009 and 2046–2065 periods but are somewhat higher for the period of 2081–2100.

4.3 Relative humidity, shortwave radiation, wind speed, and atmospheric pressure

Changes in other meteorological variables, such as relative humidity, shortwave radiation, wind speed, and atmospheric pressure are not a direct consequence of the calculated factors of change (Fatichi et al. 2011). Therefore, any inferred changes are only due to statistical and causal relationships assumed by the weather generator. Assessing magnitudes and directions of these changes and validating them with observations is an important benchmark of the

downscaling methodology. Such tests evaluate the effective capability of AWE-GEN to transfer “informed” changes of the principal variables (temperature and precipitation) to secondary effects.

Vapor pressure, or equivalently, relative humidity is an important variable for many environmental processes, e.g., it controls the process of evapotranspiration in the hydrologic cycle. Therefore, its predicted change may have non-negligible consequences. Nonetheless, near ground vapor pressure (or expressed in equivalent metrics, such as specific humidity and relative humidity) is not among conventionally archived outputs available from GCMs and the related factors of change cannot thus be directly calculated. AWE-GEN can reproduce the seasonal cycle of relative humidity highly satisfactorily for the present climate (Fig. 9a). Similar to air temperature, the BWA uncertainty bounds (the 5th and 95th percentiles) due to the stochastic variability explored for the control scenario are small and can be neglected. The predicted climate for the period of 2000–2009 captures the fundamental nature of the change, with lower relative humidity during the period of May through September and a slightly smaller relative humidity during the other months (Fig. 9b). Although the direction

of the change is well predicted, its magnitude is simulated within the envelope of the BWA ensemble members only for a few months. This suggests that the effect of climate change obtained with the stochastic downscaling is underestimated. This can be partially explained by the slight underestimation of warming (Sect. 4.2) and non-feasibility to account for large-scale climate feedbacks, since a point-scale stochastic weather generator is used. Future predictions of relative humidity show its significant decrease, especially during summer months (Fig. 9c, d). Winter months are also projected to be affected by the end of the century. An average change of -0.12 for the months of July and August is predicted, when the control scenario of 1962 through 1992 and the median of the future period of 2081 through 2100 are compared. The uncertainty of the prediction has a tendency to grow as the time interval from the control scenario increases (Fig. 9). As for air temperature, the future relative humidity simulated with the SA approach is always very close to the changes predicted with the ensemble median (with the apparent exception for July for the period of 2081–2100).

The daily cycle of relative humidity is reproduced by AWE-GEN for the control scenario quite well, especially

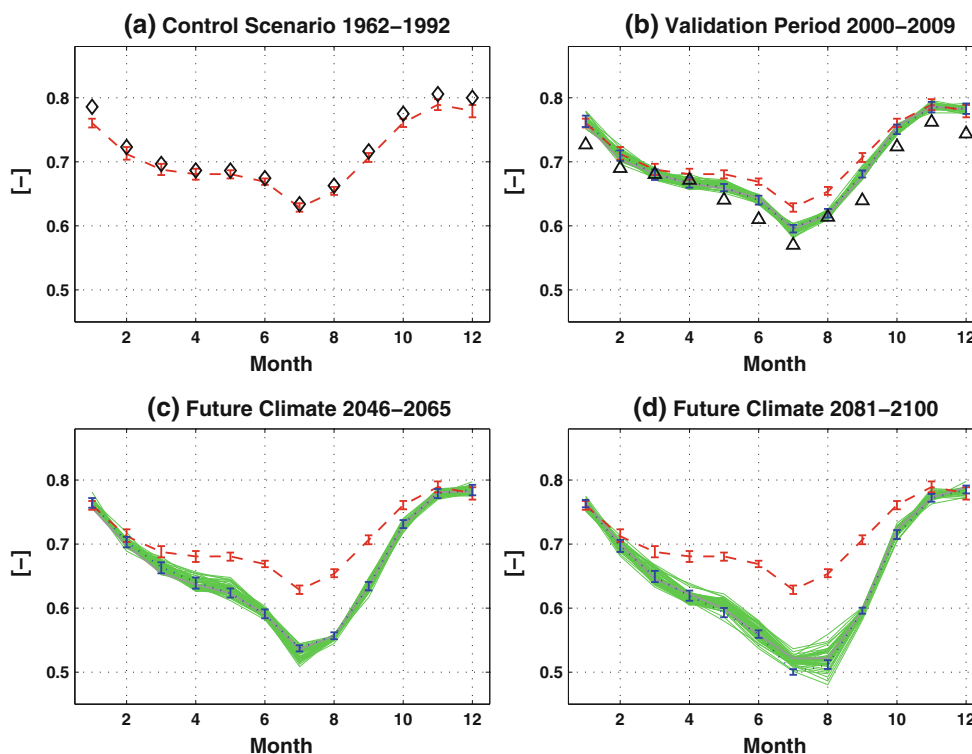


Fig. 9 Average monthly relative humidity from the observed data and simulated with the weather generator for different climate periods **a** 1962–1992, **b** 2000–2009, **c** 2046–2065, and **d** 2081–2100. The *diamonds* represent the observed values for the period of 1962–1992 (subplot **a**), and the *triangles* represent the observed values for the period of 2000–2009 (subplot **b**), the *dashed line* is the mean of the ensemble of generated climate trajectories for the control scenario,

the *vertical bars* represent the 5th and 95th percentiles (subplots **a**, **b**, **c**, and **d**), the *solid gray lines* represent the result obtained using the medians of the factors of change PDFs (subplots **b**, **c**, and **d**). The *thin green lines* represent the ensemble of climate realizations obtained with the BWA approach. The *blue dotted lines* and *blue bars* are the results of the SA simulation approach (subplots **b**, **c**, and **d**)

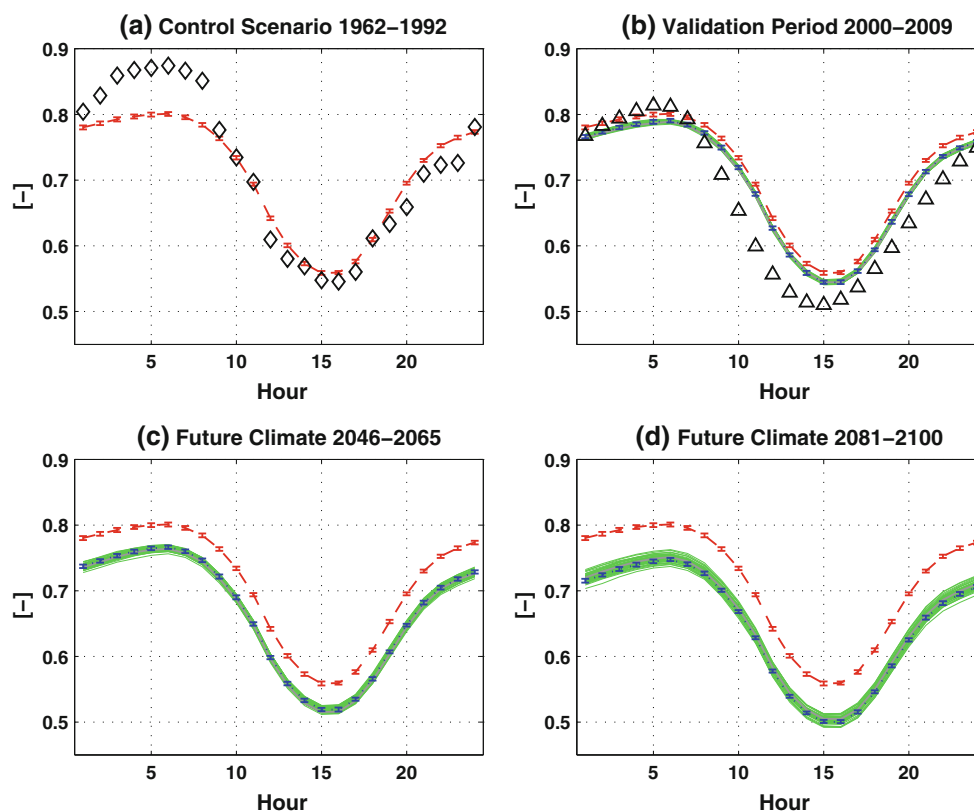


Fig. 10 The mean diurnal cycle of relative humidity from the observed data and simulated with the weather generator for different climate periods **a** 1962–1992, **b** 2000–2009, **c** 2046–2065, and **d** 2081–2100. The *diamonds* represent the observed values for the period of 1962–1992 (subplot **a**), and the *triangles* represent the observed values for the period of 2000–2009 (subplot **b**), the *dashed line* is the mean of the ensemble of generated climate trajectories for

the control scenario, the vertical bars represent the 5th and 95th percentiles (subplots **a**, **b**, **c**, and **d**), the *solid gray lines* represent the result obtained using the medians of the factors of change PDFs (subplots **b**, **c**, and **d**). The *thin green lines* represent the ensemble of climate realizations obtained with the BWA approach. The *blue dotted lines* and *blue bars* are the results of the SA simulation approach (subplots **b**, **c**, and **d**)

for the midday and late evening hours (Fig. 10a). However, similarly to the diurnal cycle of air temperature, the simulated changes are distributed evenly within a day (Fig. 10b–d). Conversely, the observed changes of daily cycle of relative humidity between the periods of 1962–1992 and 2000–2009 exhibit a diurnal pattern with a larger decrease of relative humidity during morning (hour 5–12) and almost unchanged dynamics during late evening hours (hour 16–23) (Fig. 10a, b). Fig. 10b also confirms a substantial underestimation of the change in relative humidity for the validation period of 2000 through 2009.

It should be noted that the inferred changes in relative humidity are mainly a result of changes in air temperature. This is likely to be the reason why the presented results agree well with observations, at least in terms of change patterns. Relative humidity can be transformed to vapor pressure but its changes at the monthly scale are typically minor (not shown), with the annual difference between the 1962–1992 and 2000–2009 periods equal to +38 Pa for the simulated results, and –6 Pa for observations. These

values are small and can be considered negligible. When predictions for the later periods are analyzed, the simulated mean vapor pressure tends to slightly increase: +98 Pa for the period of 2046–2065, and +134 Pa for the period of 2081–2100. This agrees with theoretical expectations of an increase in atmospheric water vapor due to the higher saturation vapor pressure of a warmer air (Held and Soden 2006; Pall et al. 2007; Lenderink and vanMeijgaard 2008; Schneider et al. 2010). Note that these predicted changes represent an outcome of imposed internal linkages among meteorological variables in AWE-GEN. They demonstrate the capability of the weather generator to effectively transfer the implication of the factors of change of precipitation and air temperature to other variables.

An assessment of performance of the stochastic downscaling methodology for shortwave radiation is not possible because the relevant observational data are only available for the period of 2000–2009. Data for this period were used to estimate the parameters of the shortwave radiation module of the weather generator. The results of the

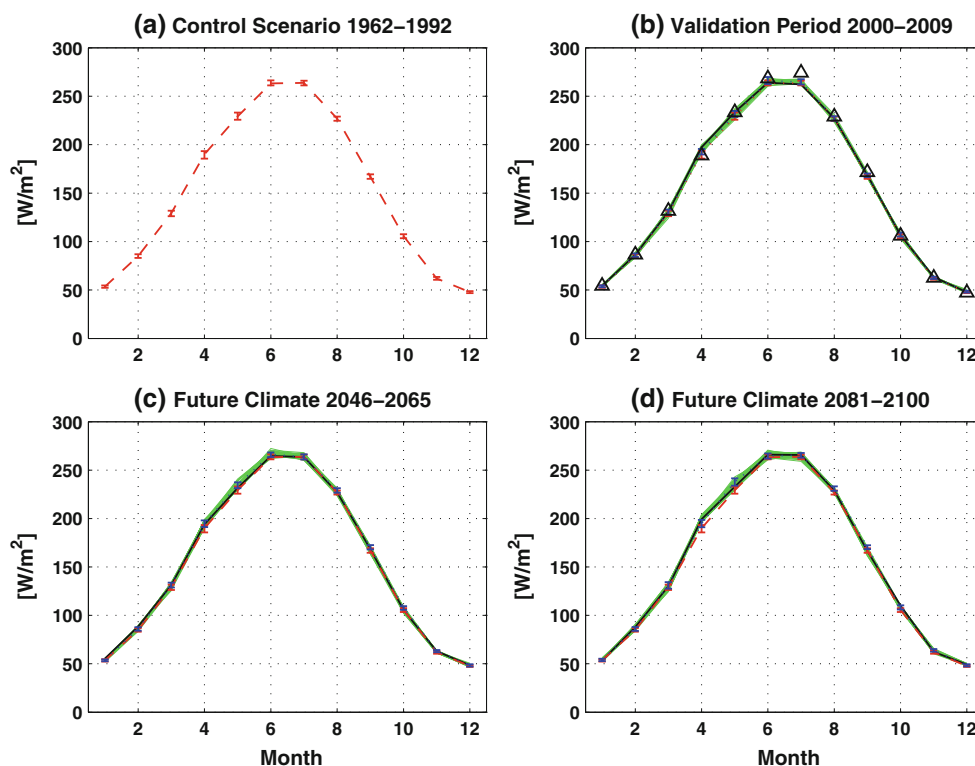


Fig. 11 Average monthly shortwave radiation from the observed data and simulated with the weather generator for different climate periods **a** 1962–1992, **b** 2000–2009, **c** 2046–2065, and **d** 2081–2100. The *triangles* represent the observed values for the period of 2000–2009 (subplot **b**), the *dashed line* is the mean of the ensemble of generated climate trajectories for the control scenario, the *vertical bars*

represent the 5th and 95th percentiles (subplots **a**, **b**, **c**, and **d**), the *solid gray lines* represent the result obtained using the medians of the factors of change PDFs (subplots **b**, **c**, and **d**). The *thin green lines* represent the ensemble of climate realizations obtained with the BWA approach. The *blue dotted lines* and *blue bars* are the results of the SA simulation approach (subplots **b**, **c**, and **d**)

simulation for the periods of 1962–1992 and 2000–2009 are shown in Fig. 11a and b. It is not surprising to observe a good performance given the fact that shortwave radiation parameters are calibrated for the 2000–2009 period. However, the effect of other meteorological variables results in a small variability of radiative flux (e.g., it is higher for the month of April in Fig. 11b). Future predictions of seasonality of shortwave radiation show very small changes (Fig. 11c and d) and a very limited range of variability among different members of the BWA ensemble. Future simulations using the SA approach yields results that are almost identical to the median of the ensemble. The relative changes of the simulated mean shortwave radiation with respect to the baseline 1962–1992 period are $+1.97 \text{ W m}^{-2}$ for the 2046–2065 period, and $+2.87 \text{ W m}^{-2}$ for the 2081–2100 period. These small variations are mainly a result of decrease in precipitation that causes a reduction of cloud cover. Such effects are accounted for by the internal structure of AWE-GEN. Other effects of climate change on radiative forcing (e.g., aerosol loading) cannot be captured by the generator with a high degree of certainty.

The simulated changes in wind speed with respect to the baseline 1962–1992 are negligible for all of the

analyzed periods, i.e., the validation and the two future periods (not shown). This simulated stationarity in the mean wind speed is not confirmed by a comparison of observations for the periods of 1962–1992 and 2000–2009. Although the presence of numerous missing values in the available time series make the analysis less robust, data show a significant increase of wind speed by $\sim 1 \text{ m s}^{-1}$. The influence of other variables on wind speed is typically small in AWE-GEN (Fatichi et al. 2011). This implies that the current approach is unable to capture any significant change in this variable. Therefore, an improvement of the stochastic downscaling methodology can be only achieved by explicitly calculating a factor of change for near ground wind speed. However, GCMs currently do not report this variable among standard outputs.

Atmospheric pressure in AWE-GEN is completely uncorrelated with other variables, therefore, the predicted change is always equal to zero. A lack of change is also confirmed by a comparison of observations for the periods of 1962–1992 and 2000–2009, over which atmospheric pressure did not show any significant change ($<1 \text{ Pa}$).

5 Discussion and conclusions

An extension of the stochastic downscaling methodology to an ensemble simulation approach has been developed and its reliability assessed. A detailed analysis of future climate predictions at the local spatial scale and hourly temporal scale has been presented by assessing climate change effects for the location of Firenze (Italy). The employed weather generator allows one to reproduce changes for different aggregation periods and meteorological variables for which the factors of change are not explicitly computed. The stochastic downscaling methodology has been corroborated by climate predictions for the period of 2000–2009 for which observations were also available. This corroboration can be regarded as a validation within the framework of stochastic simulation and, to the author's knowledge, this is a first attempt of this kind in climate downscaling studies. Note that observations for the period of 2000–2009 have been used neither for tuning or parameterizing the climate models (see Sect. 3), nor for deriving the parameters of the weather generator. These observations therefore represent relatively independent information. Although differences between the predicted and the observed changes were noted, it is argued that the presented methodology responds to the challenge quite satisfactorily.

The novelty of this study is represented by a transfer of the uncertainty of climate change predictions inferred from an ensemble of climate models to an ensemble of hourly time series representing future climate conditions. While the uncertainty derived with the presented methodology of Bayesian weighting (the BWA approach) or simple averaging (the SA approach) of multiple GCMs does not reflect all possible sources of uncertainty (for instance, it considers a single emission scenario and cannot incorporate some of climate model structural uncertainties), it represents important information for evaluations of climate change predictions (Knutti 2008; Knutti et al. 2010). Specifically, we considered three sources leading to variability in predictions: (a) the intrinsic stochasticity of climate of a “finite” 30-year period, (b) the effect of using multiple GCMs, and (c) the methodology for weighting the GCMs. In this study, weighting GCMs according to bias or convergence criteria as opposed to using equal weights was found to affect the mean signal of climate change only marginally. This is testified by the proximity of the projections, for essentially all of the climate variables, obtained with the SA approach and with the medians of the PDFs computed with the BWA approach. However, a possible added value of the Bayesian approach that permits uniform or weighted averaging of GCM realizations is the capability to summarize multi-model predictions in the form of PDFs of factors of change. Using the single factors

of change can imply a reduced uncertainty range even after accounting for the stochastic variability (Figs. 3, 4, 5). Whether such a reduced range corresponds to more accurate or too certain projections cannot be verified as yet. Consequently, the assumption of a larger uncertainty obtained with the Bayesian approach can be regarded as a conservative choice that is not “blind” to alternative scenarios of the future. Predictions in the form of PDFs are found to be very important, especially for variables such as precipitation, for which different GCMs provide varying trajectories of the change (e.g., Fig. 1). Accounting for the stochastic variability is found of paramount importance for precipitation, where stochastic variability can be compared with the climate change signal but has a negligible effect for other meteorological variables.

One of the implications of the presented approach is a possibility to assess plausibility of change of extreme precipitation in the future. We demonstrated that by using the ensemble mean or a single climate model projection as a “representative” mode of the change can lead to a significant underestimation of the range of expected future conditions or even to erroneous conclusions. The uncertainty of projections of rainfall extremes is so high that might question its practical utility. However, we believe that such methodologies nonetheless represent a step forward in capturing “vital details” of climate change (Kerr 2011).

The embedded causal and static relationships of the weather generator also allow one to obtain realistic trends and magnitudes of the change for a number of variables for which the factors of change are not directly computed (e.g., relative humidity, or higher order statistics). Accounting for this information can be important for a variety of environmental processes and management strategies. For instance, changes in the standard deviations of the daily cycle of air temperature can have important consequences in terms of temperature extremes, making very high or low temperature extremes less unusual and beyond the present historical records. This can have very important consequences for environmental processes related to temperature thresholds such as the survival of vegetation species or microorganisms.

Components of methodology where the stochastic downscaling needs improvements were also identified. While the methodology can reproduce the absolute changes of average air temperature and relative humidity fairly well, the simulated changes of the daily cycles are uniform across the day and this is not supported by the observed changes. This finding warrants efforts of archiving GCM and RCM realizations at the hourly scale, whereas the current practices make available outputs only at the daily or monthly time scales. An explicit computation of the factors of change at the hourly scale would indeed provide

a great benefit for this type of downscaling. The computation of a factor of change for wind speed is also warranted, since changes in precipitation and temperature cannot trigger changes in wind regime; observations, however, indicate that other non-local processes may alter wind magnitudes.

According to the emission scenario A1B used in this study, the practical implications of the predicted climate for the city of Firenze can be considered as significant. The changes in the precipitation regime are difficult to evaluate, given the uncertainty of stochastic realizations and climate model predictions. Yet a reduction of the total annual precipitation appears to be a consistent feature emerging from the downscaling that will be stronger during summer months for the period of 2046 through 2065, and will ultimately affect almost the entire year by the end of the twenty-first century. The median predicted change is about 14 % decrease of annual precipitation from the period of 2000–2009 to the period of 2081–2100. Similar tendencies of changes in the averages were also identified by an analysis carried out with a dynamic downscaling methodology for the entire Italian peninsula (Coppola and Giorgi 2009).

The expected change of air temperature exhibits a high confidence of an increase of about 2.5 °C by the end of the century, as compared to the 2000–2009 period, with a higher increase during summer months. The increase in air temperature leads to a significant reduction of relative humidity, especially during summer periods, because vapor pressure is predicted to increase only slightly. Solar radiation is expected to remain nearly the same across the twenty-first century exhibiting minor increments due to a reduced cloud cover.

The combination of warmer and drier conditions of future climate might have non-negligible implications for Firenze and its surrounding Tuscany countryside, in terms of water resources and natural ecosystem management, and tourism. An adaptation strategy to this expected change is therefore warranted. The discussed results were obtained accounting for the uncertainty due to biases of a multiple number of climate models. In combination with the demonstrated validation of the stochastic methodology, this allows us to conclude that the presented results can be regarded as robust estimates of climate change for the location of Firenze, given the present knowledge of climate systems (climate model realizations) and data available for downscaling.

Acknowledgments We acknowledge the modeling groups, the Program for Climate Model Diagnosis and Intercomparison (PCMDI) and the WCRP's Working Group on Coupled Modelling (WGCM) for their roles in making available the WCRP CMIP3 multi-model dataset. Support of this dataset is provided by the Office of Science, U.S. Department of Energy. Simone Fatichi gratefully acknowledges

funding from the Ente Cassa di Risparmio di Firenze with the fellowship "Jacopo Fikai" 2010 that support this research, and wishes to thank the International Ph.D. joint program on "Mitigation of Risk due to Natural Hazards on Structures and Infrastructures" between the University of Firenze (Italy) and the T.U. Braunschweig (Germany). Valeriy Yu. Ivanov was supported by the NSF grant 0911444 and NSF grant EAR 1151443.

References

- Amelung B, Nicholls S, Viner D (2007) Implications of global climate change for tourism flows and seasonality. *J Travel Res* 45(3):285–296. doi:10.1177/0047287506295937
- Anandhi A, Frei A, Pierson DC, Schneiderman EM, Zion MS, Lounsbury D, Matonse AH (2011) Examination of change factor methodologies for climate change impact assessment. *Water Resour Res* 47(W03501). doi:10.1029/2010WR009104
- Bae D-H, Jung IW, Chang H (2008) Potential changes in Korean water resources estimated by high-resolution climate simulation. *Climate Res* 35:213–226. doi:10.3354/cr00704
- Bárdossy A, Pegram G (2011) Downscaling precipitation using regional climate models and circulation patterns toward hydrology. *Water Resour Res* 47(W04505). doi:10.1029/2010WR009689
- Barnett T, Malone R, Pennell W, Stammer D, Semtner B, Washington W (2004) The effects of climate change on water resources in the west: introduction and overview. *Climatic Change* 62:1–11
- Bavay M, Lehning M, Jonas T, Löwe H (2009) Simulations of future snow cover and discharge in Alpine headwater catchments. *Hydrol Process* 23:95–108. doi:10.1002/hyp.7195
- Berrittella M, Bigano A, Roson R, Tol RSJ (2006) A general equilibrium analysis of climate change impacts on tourism. *Tour Manag* 27(5): 913–924
- Burton A, Fowler HJ, Blenkinsop S, Kilsby CG (2010) Downscaling transient climate change using a Neyman-Scott Rectangular Pulses stochastic rainfall model. *J Hydrol* 381:18–32. doi:10.1016/j.jhydrol.2009.10.031
- Christensen JH, Kjellström E, Giorgi F, Lenderink G, Rummukainen M (2010) Weight assignment in regional climate models. *Climate Res* 44:179–194. doi:10.3354/cr00916
- Christensen NS, Wood AW, Voisin N, Lettenmaier DP, Palmer RN (2004) Effects of climate change on the hydrology and water resources of the Colorado river basin. *Climatic Change* 62:337–363
- Coppola E, Giorgi F (2009) An assessment of temperature and precipitation change projections over Italy from recent global and regional climate model simulations. *Int J Climatol* 30:11–32. doi:10.1002/joc.1867
- Cunnane C (1978) Unbiased plotting positions—a review. *J Hydrol* 37:205–222
- Denis B, Laprise R, Caya D, Cote J (2002) Downscaling ability of one way nested regional climate models: the big brother experiment. *Climate Dyn* 18(8):627–646. doi:10.1007/s00382-001-0201-0
- Déqué M (2007) Frequency of precipitation and temperature extremes over France in an anthropogenic scenario: model results and statistical correction according to observed values. *Global Planet Change* 57:16–26
- Déqué M, Jones RG, Wild M, Giorgi F, Christensen JH, Hassell DC, Vidale PL, Rockel B, Jacob D, Kjellström E, de Castro M, Kucharski F, vandenHurk B (2005) Global high resolution versus Limited Area Model climate change projections over Europe: quantifying confidence level from PRUDENCE results. *Climate Dynam* 25:653–670. doi:10.1007/s00382-005-0052-1
- Deser C, Phillips A, Bourdette V, Teng H (2012) Uncertainty in climate change projections: the role of internal variability. *Climate Dynam* 38:527–546. doi:10.1007/s00382-010-0977-x

- Fatichi S (2010) The modeling of hydrological cycle and its interaction with vegetation in the framework of climate change, Ph.D. thesis, University of Firenze, Italy, and T.U. Braunschweig, Germany
- Fatichi S, Ivanov VY, Caporali E (2010) Simulating hydro-meteorological variables across a range of temporal scales with a weather generator, in International Workshop Advances in Statistical Hydrology, Taormina, Italy
- Fatichi S, Ivanov VY, Caporali E (2011) Simulation of future climate scenarios with a weather generator. *Adv Water Res* 34:448–467. doi:[10.1016/j.advwatres.2010.12.013](https://doi.org/10.1016/j.advwatres.2010.12.013)
- Fowler HJ, Wilby RL (2010) Detecting changes in seasonal precipitation extremes using regional climate model projections: implications for managing fluvial flood risk. *Water Resour Res* 46(W03525). doi:[10.1029/2008WR007636](https://doi.org/10.1029/2008WR007636)
- Fowler HJ, Blenkinsop S, Tebaldi C (2007a) Linking climate change modelling to impacts studies: recent advances in downscaling techniques for hydrological modelling. *Int J Climatol* 27:1547–1578. doi:[10.1002/joc.1556](https://doi.org/10.1002/joc.1556)
- Fowler HJ, Ekström M, Blenkinsop S, Smith AP (2007b) Estimating change in extreme european precipitation using a multimodel ensemble. *J Geophys Res* 112(D18104). doi:[10.1029/2007JD008619](https://doi.org/10.1029/2007JD008619)
- Giorgi F, Coppola E (2010) Does the model regional bias affect the projected regional climate change? An analysis of global model projections. *Climatic Change* 100:787–795. doi:[10.1007/s10584-010-9864-z](https://doi.org/10.1007/s10584-010-9864-z)
- Giorgi F, Mearns L (2003) Probability of regional climate change calculated using the reliability ensemble average (REA) method. *Geophys Res Lett* 30:1629–1632, doi:[10.1029/2003GL017130](https://doi.org/10.1029/2003GL017130)
- Groppelli B, Bocchiola D, Rosso R (2011) Spatial downscaling of precipitation from GCMs for climate change projections using random cascades: a case study in Italy. *Water Resour Res* 47(W03519). doi:[10.1029/2010WR009437](https://doi.org/10.1029/2010WR009437)
- Hawking E, Sutton R (2011) The potential to narrow uncertainty in projections of regional precipitation change. *Climate Dyn* 37:407–418. doi:[10.1007/s00382-010-0810-6](https://doi.org/10.1007/s00382-010-0810-6)
- Hay LE, Clark MP, Wilby RL, Gutowski WJ, Leavesley GH, Pan Z, Arritt RW, Takle ES (2002) Use of regional climate model output for hydrologic simulations. *J Hydrometeorol* 3:571–590
- Held IM, Soden BJ (2006) Robust responses of the hydrological cycle to global warming. *J Climate* 19:5686–5699
- Hirschi M, Stoeckli S, Dubrovsky M, Spirig C, Calanca P, Rotach MW, Fischer AM, Duffy B, Samietz J (2012) Downscaling climate change scenarios for apple pest and disease modeling in Switzerland. *Earth Syst Dyn* 3:33–47
- Hundecha Y, Bárdossy A (2008) Statistical downscaling of extremes of daily precipitation and temperature and construction of their future scenarios. *Int J Climatol* 28:589–610. doi:[10.1002/joc.1563](https://doi.org/10.1002/joc.1563)
- Ines A, Hansen J (2006) Bias correction of daily GCM rainfall for crop simulation studies. *Agric Forest Meteorol* 138:44–53
- IPCC (2000) Special report on emissions scenarios. A special Report of Working Group III of the Intergovernmental Panel on Climate Change. Cambridge University Press, Cambridge and New York, NY
- IPCC (2007) Climate change 2007: The Physical Science Basis. Contribution of Working Group I to the Fourth Assessment Report of the Intergovernmental Panel on Climate Change. Cambridge University Press, Cambridge and New York, NY
- Ivanov VY, Bras RL, Curtis DC (2007) A weather generator for hydrological, ecological, and agricultural applications. *Water Resour Res* 43:W10406. doi:[10.1029/2006WR005364](https://doi.org/10.1029/2006WR005364)
- Johnson F, Sharma A (2011) Accounting for interannual variability: a comparison of options for water resources climate change impact assessments. *Water Resour Res* 47(W04508). doi:[10.1029/2010WR009272](https://doi.org/10.1029/2010WR009272)
- Kerr RA (2011) Vital details of global warming are eluding forecasters. *Science* 334:173–174. doi:[10.1126/science.334.6053.173](https://doi.org/10.1126/science.334.6053.173)
- Kilsby CG, Jones P, Burton A, Ford A, Fowler H, Harpham C, James P, Smith A, Wilby R (2007) A daily weather generator for use in climate change studies. *Environ Model Softw* 22:1705–1719
- Knutti R (2008) Should we believe model predictions of future climate change? *Philos Trans R Soc A* 366:4647–4664. doi:[10.1098/rsta.2008.0169](https://doi.org/10.1098/rsta.2008.0169)
- Knutti R (2010) The end of model democracy? *Climatic Change* 102:395–404. doi:[10.1007/s10584-010-9800-2](https://doi.org/10.1007/s10584-010-9800-2)
- Knutti R, Furrer R, Tebaldi C, Cermak J, Meehl GA (2010) Challenges in combining projections from multiple climate models. *J Climate* 23:2739–2758
- Lambert SJ, Boer GJ (2001) CMIP1 evaluation and intercomparison of coupled climate models. *Climate Dyn* 17:83–106. doi:[10.1007/PL00013736](https://doi.org/10.1007/PL00013736)
- Leander R, Buishand TA (2007) Resampling of regional climate model output for the simulation of extreme river flows. *J Hydrol* 332:487–496. doi:[10.1016/j.jhydrol.2006.08.006](https://doi.org/10.1016/j.jhydrol.2006.08.006)
- Lefèvre RA, Sabbioni C, Centro Universitario Europeo per i Beni Culturali (2010) Climate change and cultural heritage, EDIPUGLIA. ISBN: 8872286018
- Lenderink G, van Meijgaard E (2008) Increase in hourly precipitation extremes beyond expectations from temperature changes. *Nat Geosci* 1:511–514
- Manning LJ, Hall JW, Fowler HJ, Kilsby CG, Tebaldi C (2009) Using probabilistic climate change information from a multimodel ensemble for water resources assessment. *Water Resour Res* 45(W11411), doi:[10.1029/2007WR006674](https://doi.org/10.1029/2007WR006674)
- Maraun D, Wetterhall F, Ireson AM, Chandler RE, Kendon EJ, Widmann M, Brieren S, Rust HW, Sauter T, Thomas M, Venema VKC, Chun KP, Goodess CM, Jones RG, Onof C, Vrac M, Thiele-Eich I (2010) Precipitation downscaling under climate change: recent developments to bridge the gap between dynamical models and the end user. *Rev Geophys* 48(RG3003)
- Masson D, Knutti R (2011) Climate model genealogy. *Geophys Res Lett* 38(L08703). doi:[10.1029/2011GL046864](https://doi.org/10.1029/2011GL046864)
- Meehl GA, Covey C, Delworth T, Latif M, McAvaney B, Mitchell JFB, Stouffer RJ, Taylor KE (2007a) THE WCRP CMIP3 multimodel dataset: a new era in climate change research. *Bull Am Meteorol Soc* 88:1383–1394, doi:[10.1175/BAMS-88-9-1383](https://doi.org/10.1175/BAMS-88-9-1383)
- Meehl GA, Stocker TF, Collins WD, Friedlingstein P, Gaye AT, Gregory JM, Kitoh A, Knutti R, Murphy JM, Noda A, Raper SCB, Watterston IG, Weaver AJ, Zhao ZC (2007b) Global climate projections. In: Climate change 2007: The Physical Science Basis. Contribution of working group I to the fourth assessment report of the intergovernmental panel on climate change. chap. X, Cambridge University Press Cambridge and New York, NY
- Merritt WS, Alila Y, Barton M, Taylor B, Cohen S, Neilsen D (2006) Hydrologic response to scenarios of climate change in sub watersheds of the Okanagan basin, British Columbia. *J Hydrol* 326:79–108. doi:[10.1016/j.jhydrol.2005.10.025](https://doi.org/10.1016/j.jhydrol.2005.10.025)
- Mooney H, Larigauderie A, Cesario M, Elmquist T, Hoegh-Guldberg O, Lavorel S, Mace GM, Palmer M, Scholes R, Yahara T (2009) Biodiversity, climate change, and ecosystem services. *Curr Opin Environ Sustain* 1(1):46–54
- Morin X, Thuiller W (2009) Comparing niche- and process-based models to reduce prediction uncertainty in species range shifts under climate change. *Ecology* 90:1301–1313. doi:[10.1890/08-0134.1](https://doi.org/10.1890/08-0134.1)
- Müller-Wohlfeil DI, Bürger G, Lahmer W (2000) Response of a river catchment to climate change: application of expanded downscaling to northern Germany. *Climatic Change* 47:61–89
- Pall P, Allen MR, Stone DA (2007) Testing the Clausius-Clapeyron constraint on changes in extreme precipitation under CO₂

- warming. *Climate Dyn* 28:351–363. doi:[10.1007/s00382-006-0180-2](https://doi.org/10.1007/s00382-006-0180-2)
- Peterson TC, Vose RS (1997) An overview of the global historical climatology network temperature database. *Bull Am Meteorol Soc* 78:2837–2849
- Piani C, Haerter JO, Coppola E (2009) Statistical bias correction for daily precipitation in regional climate models over Europe. *Theor Appl Climatol* 99:187–192
- Pierce DW, Barnett TP, Santer BD, Gleckler PJ (2009) Selecting global climate models for regional climate change studies. *Proc Natl Acad Sci USA* 106:8441–8446
- Prein AF, Gobiet A, Truhetz H (2011) Analysis of uncertainty in large scale climate change projections over Europe. *Meteorol Zeitschrift* 20(4):383–395, doi:[10.1127/0941-2948/2011/0286](https://doi.org/10.1127/0941-2948/2011/0286)
- Räisänen J (2007) How reliable are climate models? *Tellus A* 59:2–29. doi:[10.1111/j.1600-0870.2006.00211.x](https://doi.org/10.1111/j.1600-0870.2006.00211.x)
- Reichler T, Kim J (2008) How well do coupled models simulate today's climate? *Bull Am Meteorol Soc* 89:303–311. doi:[10.1175/BAMS-89-3-303](https://doi.org/10.1175/BAMS-89-3-303)
- Robert CP, Casella G (2010) Monte Carlo statistical methods. Springer, New York
- Schmidli J, Frei C, Vidale PL (2006) Downscaling from GCM precipitation: a benchmark for dynamical and statistical downscaling methods. *Int J Climatol* 26:679–689
- Schneider T, O’Gorman PA, Levine XJ (2010) Water vapor and the dynamics of climate changes. *Rev Geophys* 48(RG3001)
- Smith R, Tebaldi C, Nychka D, Mearns L (2009) Bayesian modeling of uncertainty in ensembles of climate models. *J Am Stat Assoc* 104(485):97–116. doi:[10.1198/jasa.2009.0007](https://doi.org/10.1198/jasa.2009.0007)
- Tebaldi C, Knutti R (2007) The use of the multi-model ensemble in probabilistic climate projections. *Philos Trans R Soc A* 365(1857):2053–2075. doi:[10.1098/rsta.2007.2076](https://doi.org/10.1098/rsta.2007.2076)
- Tebaldi C, Sansó B (2009) Joint projections of temperature and precipitation change from multiple climate models: a hierarchical Bayesian approach. *J R Stat Soc A* 172:83–106
- Tebaldi C, Mearns L, Nychka D, Smith R (2004) Regional probabilities of precipitation change: a Bayesian analysis of multimodel simulations. *Geophys Res Lett* 31(L24213). doi:[10.1029/2004GL021276](https://doi.org/10.1029/2004GL021276)
- Tebaldi C, Smith RL, Nychka D, Mearns LO (2005) Quantifying uncertainty in projections of regional climate change: A Bayesian approach to the analysis of multi-model ensembles. *J Climate* 18:1524–1540
- Thembl MJ, Gobiet A, Leuprecht A (2011) Empirical-statistical downscaling and error correction of daily precipitation from regional climate models. *Int J Climatol* 31(10):1530–1544. doi:[10.1002/joc.2168](https://doi.org/10.1002/joc.2168)
- Vrac M, Naveau P (2007) Stochastic downscaling of precipitation: from dry events to heavy rainfalls. *Water Resour Res* 43(W07402). doi:[10.1029/2006WR005308](https://doi.org/10.1029/2006WR005308)
- Vrac M, Stein ML, Hayhoe K, Liang XZ (2007) A general method for validating statistical downscaling methods under future climate change. *Geophys Res Lett* 34(L18701), doi:[10.1029/2007GL030295](https://doi.org/10.1029/2007GL030295)
- Weigel AP, Knutti R, Liniger MA, Appenzeller C (2010) Risks of model weighting in multimodel climate projections. *J Climate* 23:4175–4190. doi:[10.1175/2010JCLI3594.1](https://doi.org/10.1175/2010JCLI3594.1)
- Wilby RL, Dawson CW, Barrow EM (2002) SDSM - a decision support tool for the assessment of regional climate change impacts. *Environ Model Softw* 17(2):145–157
- Wood AW, Leung LR, Sridhar V, Lettenmaier DP (2004) Hydrologic implications of dynamical and statistical approaches to downscaling climate model outputs. *Climatic Change* 62:189–216